HOKKAIDO UNIVERSITY

Title	The effects of accumulated refractory particles and the peak inert mode temperature on semi-continuous organic carbon and elemental carbon measurements during the CAREBeijing 2006 campaign
Author(s)	Jung, Jinsang; Kim, Young J.; Lee, Kwang Yul et al.
Citation	Atmospheric Environment, 45(39), 7192-7200 https://doi.org/10.1016/j.atmosenv.2011.09.003
Issue Date	2011-12
Doc URL	https://hdl.handle.net/2115/47556
Type	journal article
File Information	AE45-39_7192-7200.pdf

Hokkaido University Collection of Scholarly and Academic Papers : HUSCAP

The effects of accumulated refractory particles and the peak inert mode temperature on semi-continuous organic carbon and elemental carbon measurements during the CAREBeijing 2006 campaign

Jinsang Jung[a,b], Young J. Kim[a,*], Kwang Yul Lee[a], Kimitaka Kawamura[b], Min Hu[c], Yutaka Kondo[d]

[a]Advanced Environmental Monitoring Research Center (ADEMRC), Gwangju Institute of Science and Technology (GIST), Gwangju, Republic of Korea

[b]Institute of Low Temperature Science, Hokkaido University, Sapporo 060-0819, Japan

[c]College of Environmental Science, Peking University, Beijing, China

[d]Research Center for Advanced Science and Technology, University of Tokyo, Tokyo, Japan

Running title: The effect of refractory particle on OC/EC measurement

Keyword: Organic carbon, Elemental carbon, Refractory particle, Pyrolyzed organic carbon, Thermal optical transmittance

Last modified: August 19, 2011

Under revision to Atmospheric Environment

*Corresponding author: Young J. Kim (yjkim@gist.ac.kr)

Abstract

Two semi-continuous Sunset carbon analyzers, with different peak inert mode temperatures (615 and 740°C), were simultaneously operated to measure fine particulate organic carbon (OC) and elemental carbon (EC) using a thermal optical transmittance method at an urban site in Beijing, China, from 16 August to 3 September 2006 during the CAREBeijing 2006 campaign. Excellent agreements were obtained between the collocated semi-continuous carbon analyzers, with slopes of 1.02 (R^2 = 0.91) for OC and 1.06 (R^2 = 0.93) for EC, resulting in very similar average EC/total carbon (TC) ratios of ~0.36. These results imply that the different peak inert mode (100% helium) temperatures did not cause significant biases on the semi-continuous OC and EC measurements. However, it was found that the EC/TC ratio was greatly influenced by the accumulated refractory particles remaining on a quartz filter ($PM_{refractory}$). Fresh quartz filters, with low $PM_{refractory}$ loadings, which is defined as a laser correction factor ≥0.94, gave ~8−10% lower EC/TC ratios than aged quartz filters with high $PM_{refractory}$ loadings. The linear regression slope between EC and optically measured EC (OPT-EC) was much higher with fresh quartz filters (slope = 1.03, R^2 = 0.96) than aged quartz filters (slope = 0.89, R^2 = 0.95), suggesting the underestimation of EC on fresh quartz filters by ~15% compared to those measured on aged quartz filters. Authentic standard humic-like substances (HULIS) on the clean quartz filter showed the highest extent of pyrolyzed organic carbon (POC) formation (47.4% in total detected carbon mass), followed by those on the Asian dust loaded quartz filter (37%) and the refractory urban pollutant loaded quartz filter (34.1%), indicating that the Asian dust and refractory urban pollutant reduced the POC

46 formation from the HULIS. Thus, this study suggested that the $PM_{refractory}$ loading
47 plays an important role in the semi-continuous OC and EC measurements by altering
48 the degree of POC formation in the inert atmosphere.

1 Introduction

Atmospheric particulate carbonaceous aerosols mainly comprises of organic (OC) and elemental carbon (EC). The thermal-optical method is a conventional approach for classifying carbonaceous aerosols into OC and EC (Huntzicker et al., 1982; Birch and Cary, 1996). OC is usually defined as carbon evolved under a prescribed temperature protocol in an inert atmosphere (100% He), while EC is defined as carbon evolved in an oxidizing atmosphere (He/10% O_2 mixture). A fraction of OC is pyrolyzed during the inert mode of the analysis. This fraction of OC is usually called pyrolyzed organic carbon (POC), quantified as the carbon evolved in the oxidizing atmosphere, which is necessary to return a laser transmittance or reflectance through a quartz filter to its initial value.

There are many uncertainties in the measurements of OC and EC, which are mainly caused by the denuder efficiency, different temperature protocols and POC correction by laser reflectance or transmittance (Schauer et al., 2003; Chow et al., 2004; Subramanian et al., 2006). Cheng et al (2010) reported that adsorbed gaseous organics (positive sampling artifact) constituted 10 and 23% of the OC concentrations during winter and summer, respectively, as determined from un-denuded quartz filter samples collected at Beijing, China. Application of a very high peak inert mode temperature (the temperature of the last step in the inert mode) may underestimate the EC concentration due to the premature evolution of EC, while a very low peak inert mode temperature may overestimate the EC concentration due to the incomplete evolution of OC in the inert atmosphere (Chow et al., 2001; Sciare et al., 2003; Schauer et al., 2003; Subramanian et al., 2006). Since POC simultaneously evolves with natural EC, as indicated by a darker color (Yang and Yu, 2002; Chow et al., 2004; Subramanian et al.,

2006), the EC values determined using a thermal/optical transmittance (TOT) method are usually lower than those using a thermal/optical reflectance (TOR) method (Chow et al., 2004; Cheng et al., 2010). Chow et al (2004) reported that the EC values determined using the TOT method were 30% lower than via the TOR method under the same temperature protocol. In order to evaluate different peak inert mode temperatures on the OC and EC measurements, previous studies have used aerosol sampling and an off-line laboratory analysis (e.g., Chow et al., 2001; Schauer et al., 2003). Thus, it is necessary to evaluate different peak inert mode temperatures on the *in-situ* on-line semi-continuous carbon analysis.

Refractory metal oxides, such as iron oxide, can cause premature EC evolution in the inert atmosphere at very high temperatures, resulting in underestimation of the EC (Polidori et al., 2006). These refractory components in the particles also caused a decrease of the laser transmittance at a high oven temperature (Huebert et al., 2004). It has been reported that ammonium bisulfate enhanced the formation of POC from starch and cellulose, but reduced their formation from levoglucosan (Yu et al., 2002). However, there have been very few studies regarding the effect of the refractory particles on the formation of POC and separation of OC and EC.

The Campaigns of Air Quality Research in Beijing and its Surrounding Regions 2006 (CAREBeijing 2006) was conducted in the summer of 2006 (e.g. Jung et al., 2009; Takegawa et al., 2009). The CAREBeijing 2006 was designed to identify the sources of ozone and aerosols in Beijing and its surrounding regions to achieve better air quality during the Beijing Olympic Games in 2008. Many research groups from China, Germany, Taiwan, Korea and Japan participated in the CAREBeijing campaign with their own instruments. Thus, this campaign was a good opportunity to compare the

97 results from different instruments operated by different research groups, which will
98 contribute to improving data quality.
99 This study investigated the semi-continuous measurements of carbonaceous aerosols
100 at two different peak inert mode temperatures (615 and 740°C). Possible reasons of the
101 disparity between the collocated semi-continuous carbon analyzers are discussed using
102 the peak inert mode temperatures and different loadings of refractory particulate matters
103 remaining on a quartz filter ($PM_{refractory}$). Clear biases in the EC/TC ratios were
104 obtained between the collocated semi-continuous carbon analyzers with respect to the
105 $PM_{refractory}$. The role of the $PM_{refractory}$ on the OC and EC measurements was
106 investigated based on the optically measured EC and the formation characteristics of
107 POC depending on the $PM_{refractory}$ loading.
108
109 **2 Experimental**
110 2.1 Description of the sampling site and campaign
111 Hourly carbonaceous particle measurements were conducted at an urban site (39.98°
112 N, 116.35° E) in Beijing from 16 August to 3 September 2006 during the CAREBeijing
113 campaign. Two Sunset semi-continuous carbon analyzers were installed on the rooftop
114 of a five-story building (~20 m above ground level) at Peking University, located in the
115 northwest of a Beijing urban area (Fig. 1). The measurement site was ~600 m north of
116 the 4th main ring road and ~220 m from the eastern main road.
117
118 2.2 Organic and elemental carbon analysis
119 Organic (OC) and elemental carbon (EC) were measured using a semi-continuous

Sunset carbon analyzer employing thermal-optical transmittance (TOT) protocol for pyrolysis correction (Birch and Cary, 1996). The air samples were drawn at 8 L per minute (LPM) through a $PM_{2.5}$ sharp-cut cyclone. The sampled aerosols then passed through a multichannel, parallel plate denuder with a carbon impregnated filter to remove semi-volatile organic vapors, and then collected on a quartz-fiber filter. OC and EC were quantified for a NDIR (non-dispersive infrared sensor) signal of CO_2 under a prescribed temperature protocol in inert (100% He) and oxidizing atmospheres (He/10% O_2 mixture), respectively. The correction of the pyrolyzed organic carbon (POC), which was converted from OC in the inert mode of the analysis, was performed by monitoring the transmittance of a pulsed He-Ne diode laser beam through the quartz fiber filter. Internal calibration was automatically performed at the end of every analysis by injecting a CH_4 internal standard mixture (5% CH_4 in He) via a fixed injection volume loop. External calibration was also performed using known amounts of sucrose. The uncertainty of the instrument was reported to be 5% (Polidori et al., 2006).

In addition to OC and EC, the semi-continuous carbon analyzer also measured the optical EC (OPT-EC) in a similar, but not identical manner to that used by the aethalometer (Jeong et al., 2004; Jung et al., 2011). The OPT-EC was calculated using a second-degree polynomial fit of the attenuation measured from the laser transmittance. The polynomial coefficients provided by the manufacturer were used in this study. Thermally measured EC and optically measured EC are further denoted as EC and OPT-EC, respectively. The total carbon (TC) was calculated by summing up OC and EC.

2.3 Temperature protocol used for OC and EC analysis

Two Sunset carbon analyzers from Gwangju Institute of Science and Technology (GIST) and Peking University together with University of Tokyo (PKU/UT) were operated in parallel and run under similar conditions, except for the temperature protocol, as shown in Table 1 (Jung et al., 2009; Han et al., 2009; Lin et al., 2009). The PKU/UT carbon analyzer used a higher He4 temperature (740°C) than the GIST carbon analyzer (615°C) (see Table 1). The PKU/UT carbon analyzer used four temperature steps (300, 450, 600 and 740°C) in the inert atmosphere for the OC analysis. After the sample had cooled, the oven temperature was increased to 870°C in the oxidizing atmosphere for the analysis of the EC and POC. However, the GIST carbon analyzer used a slightly different temperature protocol, with a lower peak temperature (615°C) in the inert atmosphere. Since most EC and POC were initially oxidized to CO_2 in the oxidizing atmosphere, an additional temperature step of 550°C was included with the GIST carbon analyzer in the oxidizing atmosphere to obtain better separation.

The peak inert mode temperature substantially influenced the EC measurements. Subramanian et al. (2006) reported that the NIOSH (National Institute for Occupational Safety and Health) peak inert mode temperature (He4-870°C) protocol measured 20-20% less EC in Pittsburgh atmospheric aerosol samples than the modified peak inert temperature (He4-700°C) protocol, while the IMPROVE (Interagency Monitoring of Protected Visual Environments) peak inert mode temperature (He4-550°C) protocol measured 50% more EC than the He4-700°C protocol for wood smoke dominated ambient samples. Schauer et al. (2003) also reported that the EC measured using the He4-550°C protocol was 1.6−2.1 times greater than that measured using the He4-870°C protocol for ambient and wood smoke samples. Polidori et al. (2006) found that the effect of metal oxides on the TOT analysis was substantially reduced when the peak

inert mode temperature was decreased from 870 to 700°C. Subramanian et al. (2006) suggested that the He4-700°C protocol provides the best estimate of the EC for the Pittsburgh samples. Thus, slightly modified peak inert mode temperatures were used in this study to minimize the measurement bias associated with the premature evolution of EC and incomplete evolution of OC in the inert atmosphere.

2.4 Blank correction and detection limit

Since the denuder cannot remove all semi-volatile organic vapors, blank correction is required for OC data. The dynamic OC blank level (positive artifact) was measured by collecting particle-free ambient air through a Teflon filter placed upstream of the denuder. The dynamic blank measurement was conducted fortnightly using the same operational protocol used for the ambient aerosol measurement. The average OC dynamic blanks were 0.94 ± 0.68 and 1.23 ± 0.43 μg C m^{-3} for the PKU/UT and GIST carbon analyzers, respectively. However, negligible EC dynamic blanks were obtained, i.e. 0.007 ± 0.01 and 0.001 ± 0.006 μg C m^{-3} for the PKU/UT and GIST carbon analyzers, respectively. These OC and EC dynamic blanks were subtracted from the raw OC and EC data.

The OC detection limits were 2.0 and 1.3 μg C m^{-3} for the PKU/UT and GIST carbon analyzers, respectively, calculated as three times the standard deviation (3σ) of the OC dynamic blank. The EC detection limits were also calculated as 3σ of the EC dynamic blank, and found to be 0.03 and 0.02 μg C m^{-3} for the PKU/UT and GIST carbon analyzers, respectively. However, these values were relatively small compared to the instrument's minimum quantifiable level given by the manufacturer, i.e. 0.5 μg C m^{-3}. Therefore, 0.5 μg C m^{-3} was considered as the EC detection limits for both semi-

192 continuous carbon analyzers. Thus, OC and EC concentrations lower than 2.0 and 0.5
193 μg C m^{-3}, respectively, were screened out in this study.
194
195 2.5 Laboratory experiments of an authentic organic standard
196 To investigate the effect of the refractory particles remaining on a quartz filter
197 ($PM_{refractory}$) on the thermal characteristics of OC and the formation of POC,
198 thermograms of an authentic organic standard were obtained in the laboratory under
199 three different sets of quartz filter conditions; baked clean quartz filter, refractory urban
200 pollutant loaded quartz filter, and Asian dust loaded quartz filter. For the filters loaded
201 with refractory urban pollutants and Asian dust, aliquots of the total suspended
202 particulate samples collected at the Gosan site, Korea (Fig. 1) during the severe long-
203 range transport pollution event (7 to 9 May 2007) and Asian dust event (30 March to 2
204 April 2007) periods, respectively, were used. Three types of the quartz filter were
205 prebaked in the Sunset carbon analyzer, using the GIST temperature protocol, to remove
206 volatile fractions from the aerosol samples, such as sulfate, nitrate, ammonium, OC and
207 EC. Thus, the term “refractory particles” in this study was defined as the particles that
208 did not vaporize under 850°C in the oxidizing atmosphere. Standard Suwannee River
209 Humic Acid (HULIS) (Cat. No: 2S101H) was obtained from the IHSS (International
210 Humic Substances Society). An aliquot (~15 μg C) of the HULIS was dissolved in ultra
211 pure organic free Milli-Q water and applied to the prebaked quartz filters using a micro
212 glass syringe and then dried over night inside a desiccator containing silica gel. The
213 prepared quartz filter samples were analyzed using the GIST temperature protocol.
214
215 **3 Results and Discussion**

3.1 Intercomparison of OC, EC, and TC between the collocated semi-continuous carbon analyzers

The TC concentrations measured by the PKU/UT and GIST carbon analyzers ranged from 2.5 to 49.5 μg C m^{-3} (AVG 18.7 ± 8.5 μg C m^{-3}) and 3.3 to 49.8 μg C m^{-3} (AVG 19.0 ± 9.2 μg C m^{-3}), respectively (Table 2), and showed excellent agreement between the two carbon analyzers, with a regression slope of 1.05 and R^2 of 0.95 (Fig. 2). The OC and EC also showed excellent agreements between the two carbon analyzers, with R^2 values > 0.92 (Fig 3a & b).

A similar intercomparison study was conducted at the Gosan site, Korea, using two semi-continuous Sunset carbon analyzers, with slightly different peak inert mode temperatures (870 and 840°C) during the Atmospheric Brown Clouds–East Asian Regional Experiment 2005 (ABC-EAREX2005) campaign (Bae et al., 2007). Poor correlation of the OC between the collocated carbon analyzers was reported, with a slope of 0.97 ± 0.07 (R^2 = 0.37), while the EC showed good agreement, with a slope of 1.05 ± 0.15 (R^2 = 0.98) (Bae et al., 2007). Our comparative result for the OC showed much better correlation, with a slope of 1.02 (R^2 = 0.91), indicating that the two different peak inert mode temperatures used in this study caused no significant bias in the OC measurement in Beijing, China. The EC also showed excellent agreement, with a slope of 1.06 (R^2 = 0.93). Since an aerosol composition, both organic and inorganic, can also influence the OC and EC measurements (Yu et al., 2002; Schauer et al., 2003), different atmospheric aerosols chemical compositions at the Gosan and Beijing may also have contributed to the difference in the OC regression results.

3.2 EC/TC ratio versus laser correction factor

The EC/TC ratios during the entire measurement period for the PKU/UT and GIST carbon analyzers ranged from 0.15 to 0.62 (AVG 0.36 ± 0.07) and from 0.18 to 0.58 (AVG 0.36 ± 0.07), respectively. It is well known that very high peak inert mode temperatures underestimate the EC and vice versa (Chow et al., 2001; Subramanian et al., 2006). Schauer et al. (2003) and Cheng et al. (2010) reported gradual decreases in the EC/TC ratios on increasing the peak inert mode temperature. Schauer et al. (2003) obtained 1.07-1.19 times differences in the EC/TC ratios measured using two different peak inert mode temperatures (650 and 750°C). The average EC/TC ratios in this study were very similar between the two carbon analyzers, suggesting that the two different peak inert mode temperatures caused no significant bias for the semi-continuous EC measurement in Beijing.

A laser correction factor was used to account for the change in the laser transmittance as a function of the temperature. This laser correction factor was calculated for each run from the variation in the laser signal on cooling of the oven after the analytical cycle had completed. The laser correction factor normally decreased as the $PM_{refractory}$ increased (Huebert et al., 2004). Thus, the laser correction factor can be used as an indicator of the aging of a quartz filter and $PM_{refractory}$ loading.

Although the average EC/TC ratios had very similar values between the two carbon analyzers, relatively poor correlation of the EC/TC ratios was obtained, with an R^2 = 0.36 (Fig. 3 and Table 2). Bae et al. (2007) also reported a similar correlation (R^2 = 0.4) between the two semi-continuous carbon analyzers at the Gosan site. Based on the assumption that the $PM_{refractory}$ may influence the OC and EC measurements, the quartz filter conditions were divided into fresh and aged quartz filters, with laser

correction factors ≥0.94 and <0.94, respectively. After omitting the EC/TC ratios with a laser correction factor ≥0.94, a better correlation of R^2 = 0.59 was obtained (Table 2), suggesting that the $PM_{refractory}$ may play an important role in the EC measurement, possibly by altering the OC/EC split point, the formation of POC, and the evolutions of EC and POC. The effects of the $PM_{refractory}$ on the EC measurements are discussed in detail in section 3.4.

The average EC/TC ratios for the two carbon analyzers are summarized in Table 3 with respect to the different laser correction factors. Clear differences in the EC/TC ratios were obtained depending on the $PM_{refractory}$ loading. The lowest EC/TC ratio of ~0.30 was obtained when the laser correction factor for the two carbon analyzers was ≥0.95. The ratio increased with increasing $PM_{refractory}$ loading, and reached ~0.38 when the laser correction factor was <0.94. By comparing the EC/TC ratios between the two carbon analyzers with different laser correction factors, it was found that fresh quartz filters with low $PM_{refractory}$ loadings gave ~8−10% lower EC/TC ratios than aged quartz filters with high $PM_{refractory}$ loadings.

3.3 Divergence of the EC measurement relative to OPT-EC

Overall, the EC and OPT-EC were well correlated, with a slope of 0.90 (R^2 = 0.94) (Fig. 4a). A relatively high regression slope of EC to OPT-EC (slope = 1.03, R^2 = 0.96) was obtained when the laser correction factor was ≥0.94 than for those under a laser correction <0.94 (slope = 0.89, R^2 = 0.95) (Table 2). A clear decreasing trend of the OPT-EC/EC ratio was observed as the laser correction factor decreased to ~0.94, and then became invariant for further decreases in the laser correction factor. These results

286 can be explained by two possible reasons; the underestimation of the EC on the fresh
287 quartz filter or the underestimation of OPT-EC on the aged quartz filter.

288 The $PM_{refractory}$ caused underestimation of the light attenuation coefficient when
289 optical carbon measurement techniques, such as an aethalometer, were used, mainly due
290 to interference via light scattering by the $PM_{refractory}$ (Weingartner et al., 2003).
291 However, this kind of interference rarely impacts on the OPT-EC data measured by the
292 Sunset carbon analyzer for the following reasons: First, if the $PM_{refractory}$ interferes
293 with the OPT-EC measurement by reducing the light attenuation coefficient, the OPT-
294 EC/EC ratio should continuously decrease as the laser correction factor decreases.
295 However, the decrease of the OPT-EC/EC ratio was only observed when the laser
296 correction factor ≥0.94, but then became invariant (Fig. 4b). Second, the Sunset carbon
297 analyzer uses a second order polynomial fit for the OPT-EC calculation from the light
298 attenuation measurement to compensate for the scattering effect due to the $PM_{refractory}$.
299 Thus, the possible underestimation of OPT-EC under high $PM_{refractory}$ loadings would
300 not be a reason for the much higher OPT-EC/EC ratios obtained for the fresh filter.
301 Rather, the underestimation of the EC for the fresh filter would more reasonably explain
302 this difference.

303 By assuming that EC on the fresh quartz filter was underestimated compared to that
304 measured from the aged quartz filter, the magnitude of the EC underestimation between
305 the fresh and aged quartz filters can be roughly estimated using the relative difference in
306 the OPT-EC/EC ratios. The OPT-EC/EC ratios were 1.09, 1.22 and 1.32 times higher
307 than those measured from the aged quartz filters when the laser correction factors were
308 0.94−0.96, 0.95−0.96 and 0.96−0.97, respectively. Thus, it was suggested that the EC

on the fresh quartz filter might be underestimated by ~15% compared that measured on the aged quartz filter. These results indicate that the $PM_{refractory}$ may play an important role in the EC measurement.

3.4 Effect of the accumulated refractory particles on the OC and EC separation

3.4.1 OC and EC split point and POC formation

The OC-EC split time is defined as the period when the laser transmittance reaches its initial value to correct for the POC formed in the inert atmosphere. The POC correction when using the thermal-optical method depends on one of the following assumptions: (i) POC evolves before the natural EC in the oxidizing atmosphere, or (ii) POC and natural EC have the same light attenuation coefficients (Yang and Yu, 2002). However, both these assumptions have been demonstrated to be invalid (Yang and Yu, 2002; Yu et al., 2002; Chow et al., 2004; Subramanian et al., 2006), which results in a systemic artifact for the split of OC and EC.

The OC-EC split times of the two carbon analyzers are shown in Fig. 5a as a function of the laser correction factor. Interestingly, the OC-EC split times gradually decreased as the laser correction factor decreased to ~0.94, and then became invariant, implying that the OC-EC split time was highly influenced by the $PM_{refractory}$. It is well known that the $PM_{refractory}$ lowers the laser transmittance through a quartz filter at high oven temperatures (Huebert et al., 2004; Polidori et al., 2006). This phenomenon was clearly observed in the CH_4 internal calibration mode, where the laser transmittance increased as the oven temperature gradually decreased. To prevent the error associated with the temperature dependent laser transmittance caused by the $PM_{refractory}$, the

Sunset manufacturer multiplies the laser correction factor by the initial laser transmittance. Thus, the difference in the OC-EC split time between the fresh and aged quartz filters cannot be explained by the temperature dependence of the laser transmittance.

To examine the effect of shifting the OC-EC split time on the amount of POC evolved in the oxidizing atmosphere, the POC/(POC+EC) ratios were plotted as a function of the laser correction factor, as shown in Fig. 5b. The decreasing trend of the POC/(POC+EC) ratios with decreasing laser correction factor was similar to that of the OC-EC split time (Fig. 5a). The POC/(POC+EC) ratios sharply decreased from 0.46 to 0.11 as the laser correction factor decreased from 0.96−0.97 to 0.92−0.94 for the PKU/UT carbon analyzer, and from 0.49 to 0.17 for the GIST carbon analyzers. The ratios were then slightly decreased with laser correction factors between 0.94 and 0.84, as shown in Fig. 5b. Much higher POC/(POC+EC) ratios with laser correction factors $\geq$0.94 were observed than with those <0.94, suggested the enhanced formation of POC on the fresh quartz filter. A decrease in the POC/(POC+EC) ratio with decreasing laser correction factor may also be attributable to the premature evolution of EC in the inert atmosphere due to mineral oxides, such as iron oxide, remaining on the quartz filter, which promotes the catalytic oxidation of carbon on the filter in the inert atmosphere (Polidori et al., 2006).

3.4.2 Thermograms of the fresh quartz filter versus high loadings of refractory particles

Figure 6 shows thermograms for selected samples (19 August 2006, 13:00 and 27 August 2006, 23:00) obtained by the PKU/UT and GIST carbon analyzers. The fresh

and aged quartz filters on 19 August 2006, 13:00 for the PKU/UT and GIST carbon analyzers represent laser correction factors of 0.956 and 0.909, respectively. Those on 27 August 2006, 23:00 for the GIST and PKU/UT carbon analyzers represent correction factors of 0.958 and 0.911, respectively. The thermograms showed that a dominant fraction of OC evolved in the He1 temperature step for the two carbon analyzers, followed by the He2 temperature step. As previously discussed for Fig. 5a, the OC-EC split time with the aged quartz filter appeared earlier than that with the fresh quartz filter.

Increases in the laser transmittance at the peak inert mode temperature (He4) were clearly observed with the aged quartz filters for the two carbon analyzers, indicating that the earlier OC-EC split time with the aged quartz filter may be partially attributable to the premature evolution of EC. However, no big difference in the CO_2 areas was observed between the fresh and aged quartz filters in the He4 temperature step. Since POC simultaneously evolves with natural EC, if the OC-EC split point does not occur in the inert atmosphere, the premature evolution of EC would not affect the EC measurement. However, clear differences in EC/TC ratios were reported for the different peak inert mode temperatures used in previous studies (e.g. Schauer et al., 2003; Subramanian et al., 2006). These differences can be explained by the different vaporization rates of natural EC and POC between the peak inert mode and the oxidizing atmosphere, as described by Subramanian et al. (2006). However, our results showed very similar average EC/TC ratios for the aged quartz filters between the two peak inert mode temperatures (Table 2), suggesting that the premature evolution of EC did not significantly affect the semi-continuous EC measurement in Beijing. Thus, the difference in EC/TC ratios between the fresh and aged quartz filters may have been caused by the premature evolution of EC as well as other reasons.

Interestingly, it was clear that the POC formation able to be monitored by the reduced laser transmittance was quite different between the fresh and aged filters. The POC formation on the fresh quartz filter was quite noticeable in the He1 temperature step for the two carbon analyzers, where the dominant fraction of OC evolved. However, the enhanced formation of POC was observed in the He2 temperature step for the aged quartz filter. These results imply that the $PM_{refractory}$ may alter the POC formation mechanism.

Most of the EC and POC evolved at the beginning of the first step of the oxidizing atmosphere (Fig. 6). Small uncertainties in the laser transmittance signal and transit time correction (the time used to correct the differences in the laser signal and CO_2 response) can cause high uncertainties in the EC measurement. The intermediate temperature step (550 °C) in the oxidizing atmosphere (Fig. 6a) gave better separation than the one-step temperature (870°C) protocol (Fig. 6b), which would help to reduce the uncertainties associated with the fluctuation in the laser signal and the error in the transit time correction, which is the time required for CO_2 generated from a sample to reach the NDIR.

3.4.3 Laboratory experiments on the formation of POC with and without refractory particles

To investigate the relatively low EC/TC ratios on the fresh quartz filter compared to those on the aged quartz filter (Figs. 3−4), the authentic standard HULIS was analyzed under three different sets of quartz filter conditions; clean quartz filter, the refractory urban pollutant loaded quartz filter and the Asian dust loaded quartz filter, to examine

403 the role of $PM_{refractory}$ on the OC and EC measurements (Fig. 7). Relatively low
404 evolutions of OC in the He2, He3 and He4 temperature steps were obtained in the range
405 of 11.5% − 22.1% (% of the evolved carbon mass in total detected carbon mass) with
406 the clean quartz filter compared to the quartz filters loaded with refractory urban
407 pollutants (16.7% − 28.1%) and the Asian dust (16.7% − 25.8%). Interestingly, the
408 HULIS on the clean quartz filter showed the highest degree of POC formation (47.4%),
409 followed by the Asian dust loaded filter (37%) and the refractory urban pollutant loaded
410 filter (34.1%). These results indicated that the Asian dust and refractory urban pollutants
411 reduced the POC formation from the HULIS. The HULIS on the refractory urban
412 pollutant loaded quartz filter and the Asian dust loaded filter showed similar evolution
413 patterns, with the exception of slight differences in the He1 and He2 temperature steps.
414 Since the attenuation coefficient of POC was ~2 times higher than that of natural EC,
415 as well as their simultaneous evolution (Yang and Yu, 2002; Chow et al., 2004;
416 Subramanian et al., 2006), a relatively high degree of POC formation on the clean
417 quartz filter would require the evolution of more EC in the oxidizing atmosphere until
418 the laser transmittance returned to its initial value, causing underestimation of the EC.
419 Thus, relatively low EC/TC ratios and high OPT-EC/EC ratios for the fresh quartz filter
420 were observed compared to those for the aged quartz filters, which were mainly
421 attributed to the variations in the POC formation caused by the $PM_{refractory}$.
422
423 ## 4 Conclusion
424 Schauer et al. (2003) reported higher EC/TC ratios (~1.07 − 1.19 times) at the peak
425 inert mode temperature of 650°C than those at 750°C based on aerosol filter sampling

and off-line laboratory analyses using the thermal optical transmittance method. However, the present study showed very similar average EC/TC ratios between the collocated semi-continuous carbon analyzers with two different peak inert mode temperatures (615 and 740°C), suggesting that the peak inert mode temperature did not cause significant bias in the semi-continuous EC measurements. The standard humic-like substance (HULIS) on the clean quartz filter showed the highest degree of formation of pyrolyzed organic carbon (POC) (47.4% of the total detected carbon mass), followed by the quartz filters loaded with Asian dust (37%) and the refractory urban pollutants (34.1%). Relatively high POC formation on the clean quartz filter would require to evolution of more EC in the oxidizing atmosphere until the laser transmittance returned to its initial value, causing underestimation of the EC. Thus, the relatively low EC/TC ratios and high OPT-EC/EC ratios for the fresh quartz filter (laser correction factor $\geq$0.94) compared to those for the aged quartz filter (laser correction factor <0.94) were mainly attributed to variations in the formation of POC due to the accumulated refractory particles remaining on the quartz filters. Since the effect of the refractory particles on the formation of POC may also depend on the chemical composition of organic aerosols, further studies are needed during different seasons and at various locations.

Acknowledgement

This work, as part of CAREBeijing 2006 (Campaign of Atmospheric REsearches in Beijing and surrounding areas in 2006), was supported by Beijing Council of Science and Technology (HB200504-6, HB200504-2), and by a National Research Foundation

of Korea (NRF) grant funded by the Korea government (MEST) (No. 2008-0060618). This work was also supported by a Grant-in-Aid, No. 2100923509, from the Japan Society for the Promotion of Science (JSPS). We appreciate the financial support of a JSPS Fellowship to J. S. Jung.

455 **Reference**

456 Bae, M. S., Hong, C. S., Kim, Y. J., Han, J. S., Moon, K. J., Kondo, Y., Komazaki, Y.,
457 Miyazaki, Y., 2007. Intercomparison of two different thermal-optical elemental
458 carbons and optical black carbon during ABC-EAREX2005. Atmospheric
459 Environment 41, 2791−2803.
460 Birch, M. E., Cary, R. A., 1996. Elemental Carbon-Based Method for Monitoring
461 Occupational Exposures to Particulate Diesel Exhaust. Aerosol Science and
462 Technology 25, 221−241.
463 Cheng, Y., He, K. B., Duan, F. K., Zheng, M., Ma, Y. L., Tan, J. H., Du, Z. Y., 2010.
464 Improved measurement of carbonaceous aerosol: evaluation of the sampling
465 artifacts and inter-comparison of the thermal-optical analysis methods. Atmospheric
466 Chemistry and Physics 10, 8533–8548.
467 Chow, J. C., Watson, J. G., Crow, D., Lowenthal, D. H., Merrifield, T., 2001.
468 Comparison of IMPROVE and NIOSH carbon measurements. Aerosol Science and
469 Technology 34, 23–34.
470 Chow, J. C., Watson, J. G., Chen, L. A., Arnott, W. P., Moosmüller, H., 2004.
471 Equivalence of elemental carbon by thermal/optical reflectance and transmittance
472 with different temperature protocols. Environmental Science & Technology 38,
473 4414–4422.
474 Han, S., Kondo, Y., Oshima, N., Takegawa, N., Miyazaki, Y., Hu, M., Lin, P., Deng, Z.,
475 Zhao, Y., Sugimoto, N., Wu, Y., 2009. Temporal variations of elemental carbon in
476 Beijing. Journal of Geophysical Research 114, D23202, doi:10.1029/2009JD012027.
477 Huebert, B., Bertram, T., Kline, J., Howell, S., 2004. Measurements of organic and
478 elemental carbon in Asian outflow during ACE-Asia form NSF/NCAR C-130.

Journal of Geophysical Research 109, D19S11, doi:10.1029/2004JD004700.

Huntzicker, J. J., Johnson, R. L., Shah, J. J., Cary, R. A., 1982. Analysis of organic and elemental carbon in ambient aerosols by a thermal-optical method. Particulate carbon: atmospheric life cycle. edited by: Wolff, G. T. and Klimisch, R. L., Plenum Press, New York, 79–85.

Jeong, C. H., Hopke, P. K., Kim, E., Lee, D. W., 2004. The comparison between thermal-optical transmittance elemental carbon and Aethalometer black carbon measured at multiple monitoring sites. Atmospheric Environment 38, 5193–5204.

Jung, J., Lee, H. L., Kim, Y. J., Liu, X., Liu, X., Zhang, Y., Hu, M., Sugimoto, M., 2009. Optical Properties of Atmospheric Aerosols Obtained by In-situ and Remote Measurements during 2006 CAREBEIJING Campaign. Journal of Geophysical Research 114, D00G02, doi:10.1029/2008JD010337.

Jung, J., Kim, Y. J., 2011. Tracking sources of severe haze episodes and their physico-chemical and hygroscopic properties under Asian continental outflow: Long-range transport pollution, post-harvest biomass burning, and Asian dust. Journal of Geophysical Research, 116, D02206, doi:10.1029/2010JD014555

Lin, P., Hu, M., Deng, Z., Slanina, J., Han, S., Kondo, Y., Takegawa, N., Miyazaki, Y., Zhao, Y., Sugimoto, N., 2009. Seasonal and diurnal variations of organic carbon in PM2.5 in Beijing and the estimation of secondary organic carbon. Journal of Geophysical Research 114, D00G11, doi:10.1029/2008JD010902.

Polidori, A., Turpin, B. J., Lim, H-J., Cabada, J. C., Subramanian, R., Pandis, S. N., Robinson A. L., 2006. Local and Regional Secondary Organic Aerosol: Insights from a Year of Semi-Continuous Carbon Measurements at Pittsburgh. Aerosol Science and Technology 40, 861–872.

503 Schauer, J. J., Mader, B. T., DeMinter, J. T., Heidemann, G., Bae, M. S., Seinfeld, J. H.,
504 Flagan, R, C., Cary, R. A., Smith, D., Huebert, B. J., Bertram, T., Howell, S., Kline,
505 J. T., Quinn, P., Bates, T., Turpin, B., Lim, H. J., Yu, J. Z., Yang, H., Keywood, M.
506 D., 2003. ACE-Asia intercomparison of a thermal-optical method for the
507 determination of particle-phase organic and elemental carbon. Environmental
508 Science & Technology 37, 993–1001.
509 Sciare, J., Cachier, H., Oikonomou, K., Ausset, P., Sarda-Estéve, R., Mihalopoulos, N.,
510 2003. Characterization of carbonaceous aerosols during the MINOS campaign in
511 Crete, July–August 2001: a multi-analytical approach. Atmospheric Chemistry &
512 Physics 3, 1743–1757.
513 Subramanian, R., Khlystov, A. Y., Robinson, A. L., 2006. Effect of peak inert-mode
514 temperature on elemental carbon measured using thermal-optical analysis. Aerosol
515 Science and Technology 40, 763–780.
516 Takegawa, N., Miyakawa, T., Kuwata, M., Kondo, Y., Zhao, Y., Han, S., Kita, K.,
517 Miyazaki, Y., Deng, Z., Xiao, R., Hu, M., van Panxteren, D., Herrmann, H.,
518 Hofzumanhaus, A., Holland, F., Wahner, A., Blake, D. R., Sugimoto, N., Zhu, T.,
519 2009. Variability of submicron aerosol observed at a rural site in Beijing in the
520 summer of 2006. Journal of Geophysical Research 114, D00G05,
521 doi:10.1029/2008JD010857.
522 Weingartner, E., Saatho, H., Schnaiter, M., Streit, N., Bitnar, B., Baltensperger, U., 2003.
523 Absorption of light by soot particles: determination of the absorption coefficient by
524 means of aethalometers. Journal of Aerosol Science 34, 1445–1463.
525 Yang, H., Yu, J. Z., 2002. Uncertainties in charring correction in the analysis of
526 elemental and organic carbon in atmospheric particles by thermal/optical methods.

527 Environmental Science & Technology 36, 5199–5204.
528 Yu, J. Z., Xu, J. H., Yang, H., 2002. Charring characteristics of atmospheric organic
529 particulate matter in thermal analysis. Environmental Science & Technology 36,
530 754–761.

531 Table 1. Temperature protocols for the OC/EC instruments used during the
532 CAREBeijing 2006 campaign.

Carrier gas	Carbon fraction	GIST[a)]		PKU/UT[b)]	
		Oven Temp (°C)	Holding time	Oven Temp (°C)	Holding time (sec)
He		-	10	-	300
He (He1)	OC1	310	60	300	75
He (He2)	OC2	480	60	450	60
He (He3)	OC3	550	60	600	60
He (He4)	OC4	615	90	740	90
He		cool down	35	cool down	30
10% O_2/He	EC1	550	35	870	120
10% O_2/He	EC2	850	105		

533 [a)]Thermal optical transmittance method, GIST: Gwangju Institute of Science and
534 Technology, Korea.
535 [b)]Thermal optical reflectance method, PKU: Peking University, China, UT: University
536 of Tokyo, Japan
537

538 Table 2. Regression analyses between the two semi-continuous carbon analyzers.

Parameter	X versus Y	R^2	Slope	Intercept	AVG X	AVG Y
					μg C m^{-3}	
TC	PKU/UT vs. GIST	0.95	1.05	-0.7	18.7 ± 8.5	19.0 ± 9.2
OC	PKU/UT vs. GIST	0.91	1.02	-0.2	12.0 ± 5.5	12.0 ± 5.9
EC	PKU/UT vs. GIST	0.93	1.06	-0.2	6.7 ± 3.3	6.9 ± 3.7
EC/TC ratio	PKU/UT vs. GIST	0.36	0.97	0[a)]	0.36 ± 0.07	0.36 ± 0.07
	PKU/UT vs. GIST (laser corr[b)] <0.94)	0.59	0.96	0[a)]	0.37 ± 0.07	0.38 ± 0.07
GIST EC vs OPT-EC	EC vs. OPT-EC (laser corr < 0.94)	0.95	0.89	0.3	7.3 ± 3.7	6.8 ± 3.4
	EC vs. OPT-EC (laser corr ≥0.94)	0.96	1.03	0.2	5.3 ± 3.2	5.8 ± 3.3

539 [a)]Intercept was forced through zero.
540 [b)]laser corr: laser correction factor used to account for the change in a laser
541 transmittance as a function of the temperature.
542

543 Table 3. Average EC/TC ratios in the two carbon analyzers with respect to the laser
544 correction factor.

Laser correction factor	Average EC/TC ratio	
	GIST	PKU/UT
All	0.36 ± 0.07	0.36 ± 0.07
GIST ≥ 0.94 and PKU/UT < 0.94	0.34 ± 0.07	0.38 ± 0.07
GIST < 0.94 and PKU/UT ≥ 0.94	0.38 ± 0.06	0.35 ± 0.08
GIST ≥ 0.95	0.30 ± 0.07	
PKU/UT ≥ 0.95		0.30 ± 0.08

List of Figures

Figure 1. Map of the measurement site (39.98 °N 116.35 °E) in Beijing, China during the CAREBeijing 2006 campaign, located in the northwest of a Beijing urban area.

Figure 2. Scatter plots of the fine carbonaceous aerosols between the collocated semi-continuous carbon analyzers for (a) organic carbon (OC) and (b) elemental carbon (EC). Please see Table 1 for abbreviations.

Figure 3. Scatter plots of EC/TC ratios obtained from the collocated semi-continuous carbon analyzers. The colored bars represent the laser correction factor for (a) the GIST and (b) PKU/UT carbon analyzers.

Figure 4. (a) Scatter plots of EC versus optically measured EC (OPT-EC) measured by the GIST carbon analyzer and (b) OPT-EC/EC ratios as a function of the laser correction factor.

Figure 5. (a) OC-EC split times of the PKU/UT and GIST carbon analyzers and (b) pyrolyzed organic carbon (POC) to the total EC evolved in the oxidizing atmosphere (sum of POC and EC) as a function of the laser correction factor. Red rectangles and black diamonds represent the data obtained from the PKU/UT and GIST carbon analyzers, respectively.

Figure 6. Thermograms for the (a) GIST and (b) PKU/UT carbon analyzers measured on 19 August 2006 at 13:00 and 27 August 2006 at 23:00. Red and blue colors represent the fresh (laser correction factor $\geq$0.94) and aged quartz filters (laser correction factor <0.94), respectively.

Figure 7. Thermograms for the standard humic-like substances (HULIS) with three different quartz filters: the clean quartz filter (blue), the refractory urban pollutant loaded quartz filter (black) and the Asian dust loaded quartz filter (red).

Figure 1

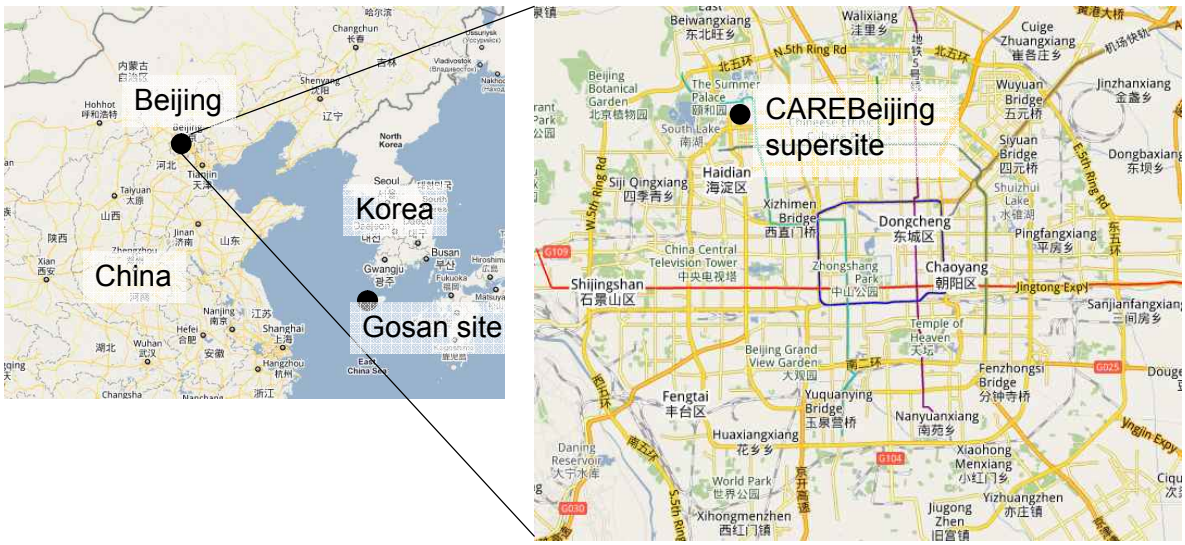
Beijing
China
Korea
Gosan site
CAREBeijing
supersite
Beiwangxiang
东北旺乡
Walixiang
洼里乡
Cuige
Zhuangxiang
崔各庄乡
N.5th Ring Rd
北五环
Beijing
Botanical
Garden
北京植物园
The Summer
Palace
颐和园
South Lake
南湖
Wuyuan
Bridge
五元桥
Jinzhanxiang
金盏乡
Siyuan
Bridge
四元桥
Dongbaxiang
东坝乡
Siji Qingxiang
四季青乡
Haidian
海淀区
W.5th Ring Rd
E.5th Ring Rd
Xizhimen
Bridge
西直门桥
Dongcheng
东城区
Shuizhui
Lake
水碓湖
Pingfangxiang
平房乡
东五环
G109
China Central
Television Tower
中央电视塔
Zhongshang
Park
中山公园
Chaoyang
朝阳区
Shijingshan
石景山区
Jingtong Expy
Sanjianfangxiang
三间房乡
Temple of
Heaven
天坛
Beijing Grand
View Garden
大观园
南二环
Fenzhongsi
Bridge
分钟寺桥
G025
Douge
Fengtai
丰台区
Yuquanying
Bridge
玉泉营桥
Nanyuanxiang
南苑乡
Huaxiangxiang
花乡乡
Yinglin Expy
Daning
Reservoir
大宁水库
南五环
G104
Xiaohong
Menxiang
小红门乡
World Park
世界公园
京开高速
S.5th Ring Rd
G030
Xihongmenzhen
西红门镇
Jiugong
Zhen
旧宫镇
Yizhuangzhen
亦庄镇

Figure 2

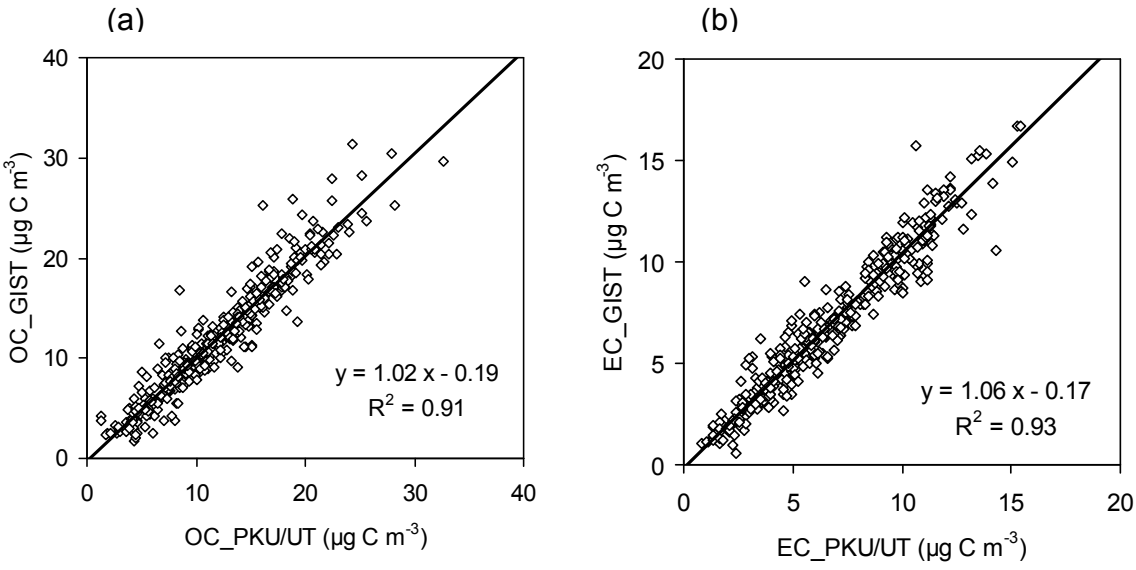
(a)
OC_GIST (μg C m-3)
OC_PKU/UT (μg C m-3)
y = 1.02 x - 0.19
R2 = 0.91
0
10
20
30
40
(b)
EC_GIST (μg C m-3)
EC_PKU/UT (μg C m-3)
y = 1.06 x - 0.17
R2 = 0.93
0
5
10
15
20

Figure 3

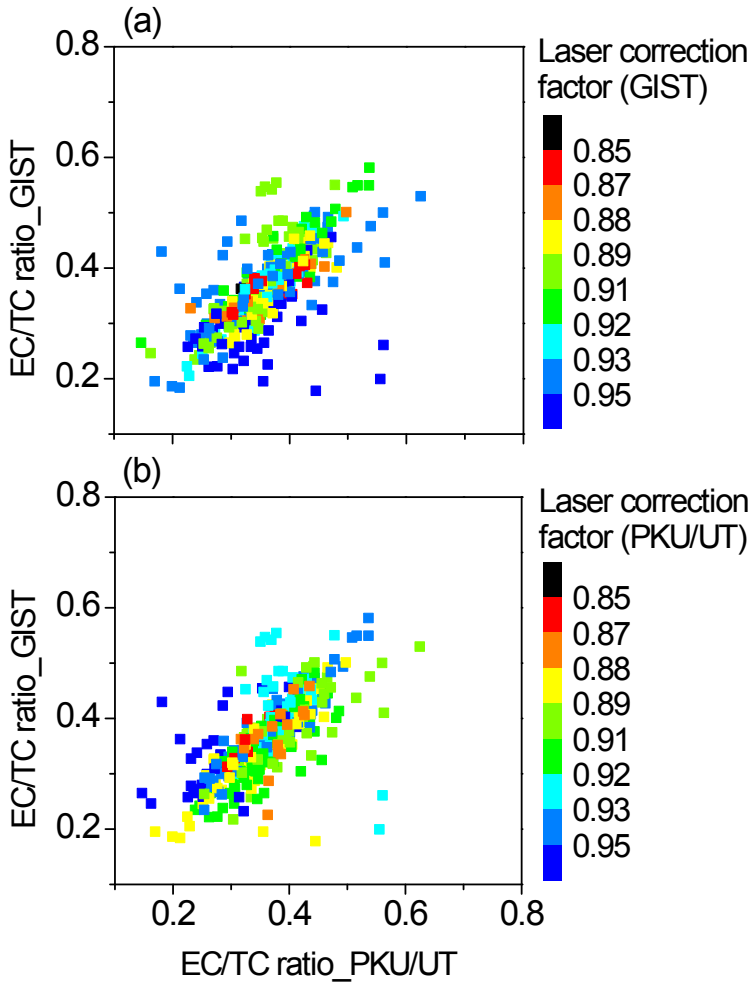
(a)
0.8
0.6
0.4
0.2
EC/TC ratio_GIST
Laser correction factor (GIST)
0.85
0.87
0.88
0.89
0.91
0.92
0.93
0.95
(b)
0.8
0.6
0.4
0.2
EC/TC ratio_GIST
Laser correction factor (PKU/UT)
0.85
0.87
0.88
0.89
0.91
0.92
0.93
0.95
0.2
0.4
0.6
0.8
EC/TC ratio_PKU/UT

Figure 4

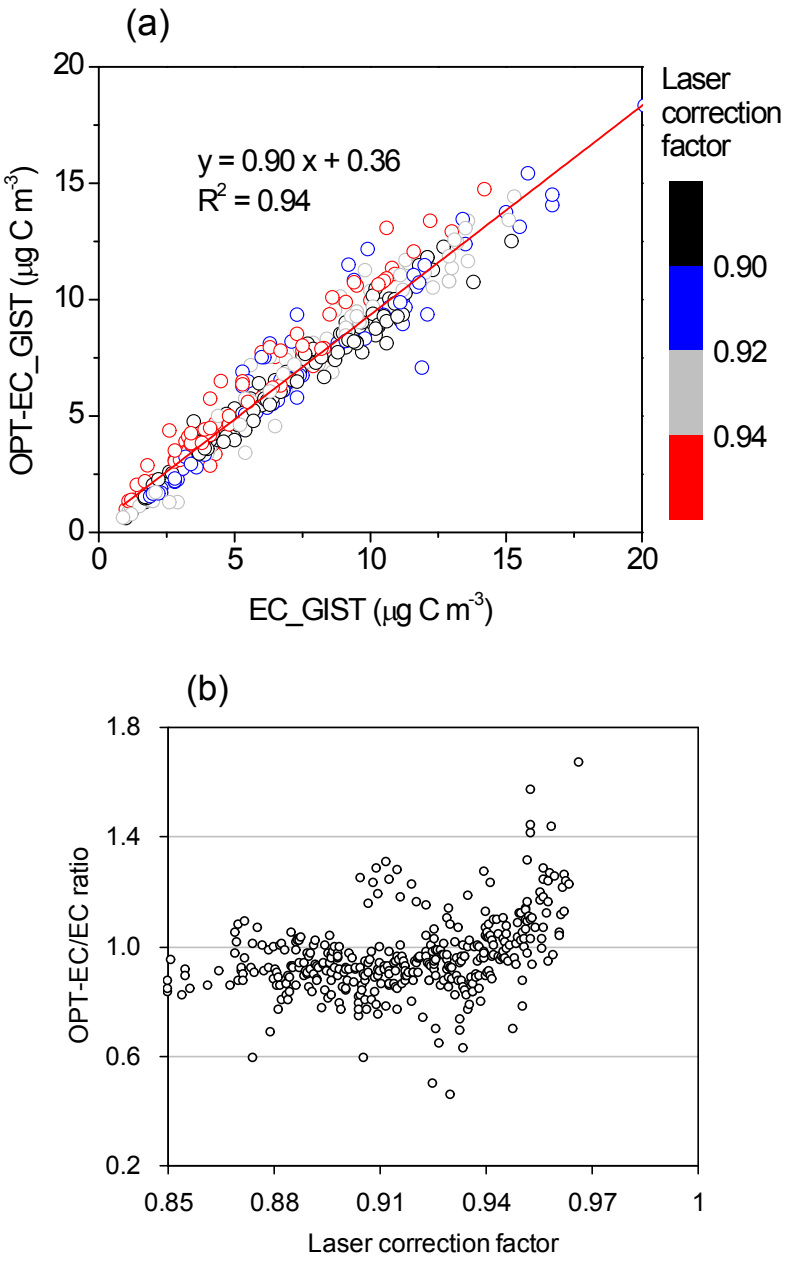
(a)
y = 0.90 x + 0.36
R2 = 0.94
OPT-EC_GIST (µg C m-3)
EC_GIST (µg C m-3)
Laser correction factor
0.90
0.92
0.94
0
5
10
15
20
(b)
OPT-EC/EC ratio
Laser correction factor
0.2
0.6
1.0
1.4
1.8
0.85
0.88
0.91
0.94
0.97
1

Figure 5

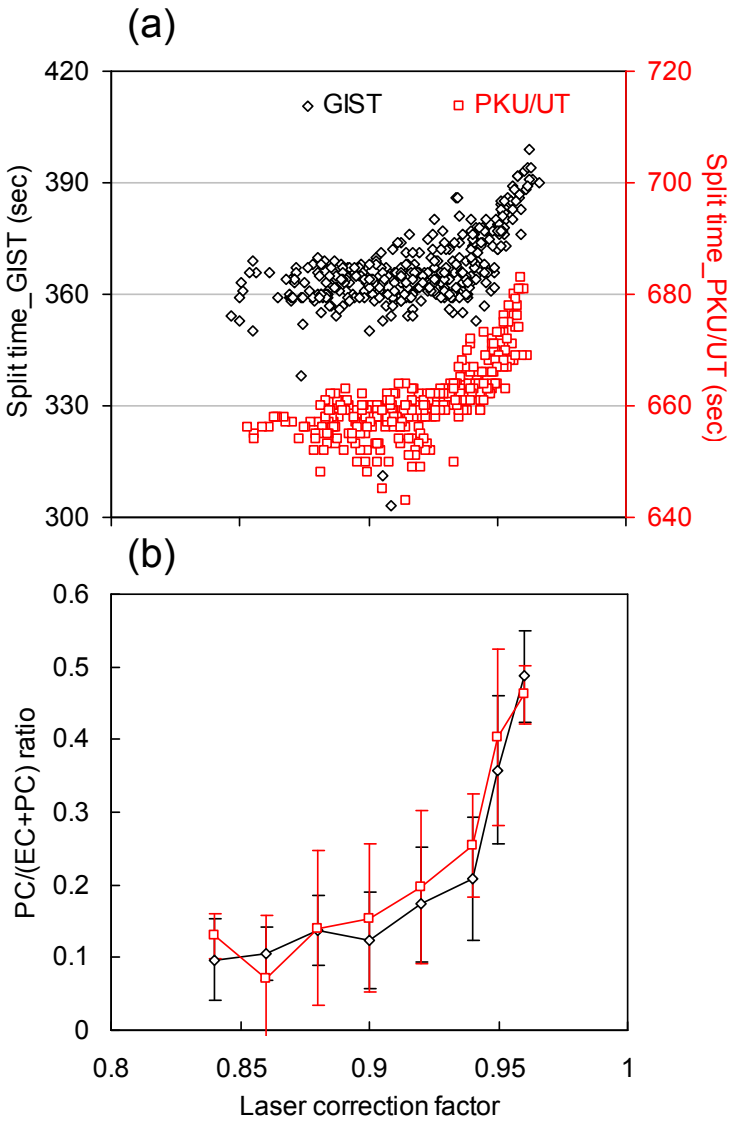
(a)
GIST
PKU/UT
Split time_GIST (sec)
Split time_PKU/UT (sec)
420
390
360
330
300
720
700
680
660
640
(b)
PC/(EC+PC) ratio
0.6
0.5
0.4
0.3
0.2
0.1
0
0.8
0.85
0.9
0.95
1
Laser correction factor

Figure 6

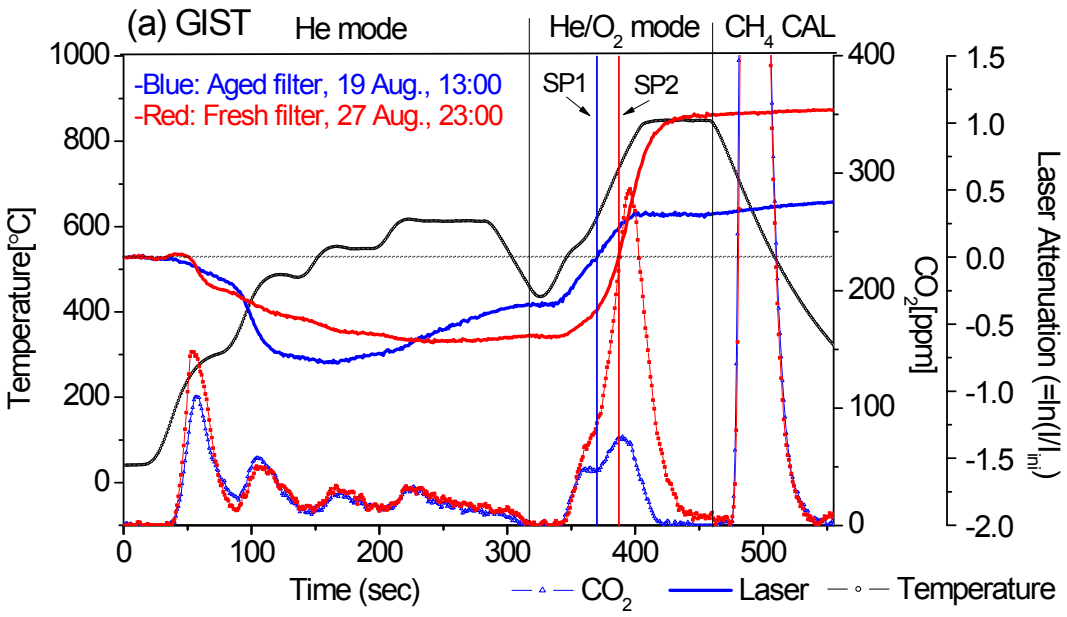
(a) GIST
He mode
He/O2 mode
CH4 CAL
-Blue: Aged filter, 19 Aug., 13:00
-Red: Fresh filter, 27 Aug., 23:00
SP1
SP2
Temperature[°C]
CO2[ppm]
Laser Attenuation (=ln(I/Iini))
Time (sec)
CO2
Laser
Temperature

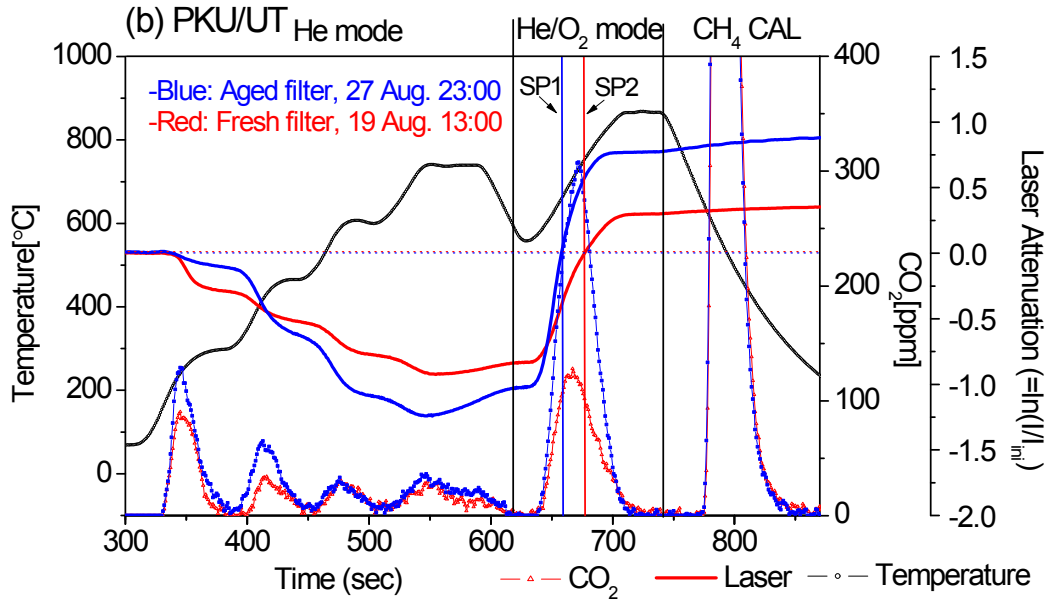
(b) PKU/UT
He mode
He/O2 mode
CH4 CAL
-Blue: Aged filter, 27 Aug. 23:00
-Red: Fresh filter, 19 Aug. 13:00
SP1
SP2
Temperature[°C]
CO2[ppm]
Laser Attenuation (=ln(I/Iini))
Time (sec)
CO2
Laser
Temperature

Figure 7

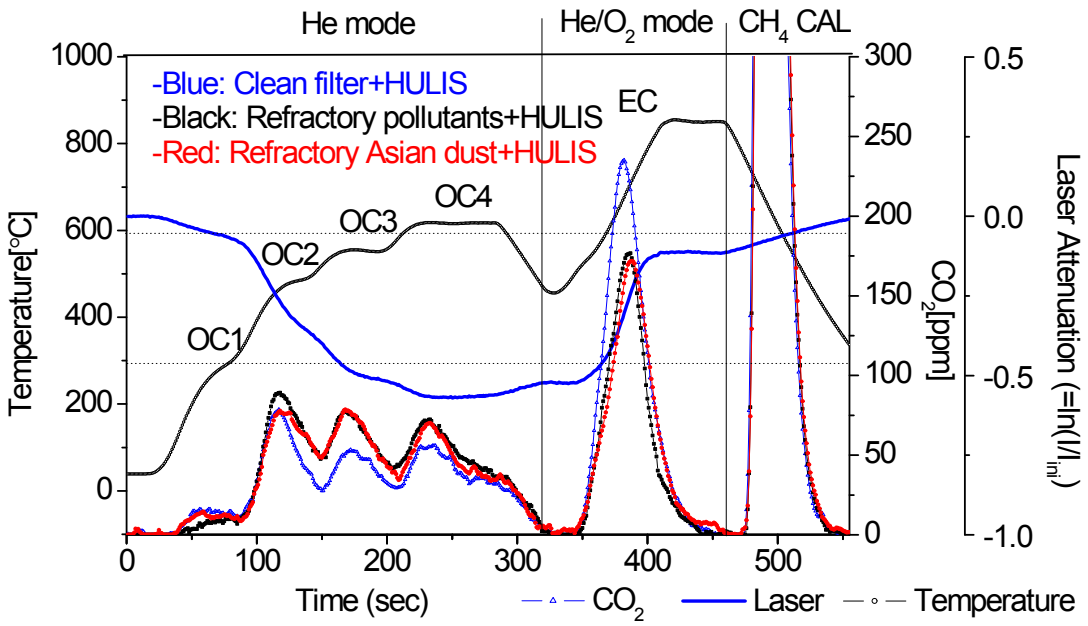
He mode
He/O2 mode
CH4 CAL
-Blue: Clean filter+HULIS
-Black: Refractory pollutants+HULIS
-Red: Refractory Asian dust+HULIS
EC
OC4
OC3
OC2
OC1
Temperature[°C]
CO2[ppm]
Laser Attenuation (=ln(I/Iini))
Time (sec)
CO2
Laser
Temperature